

Mesencephalic Astrocyte–Derived Neurotrophic Factor as a Urine Biomarker for Endoplasmic Reticulum Stress–Related Kidney Diseases

Yeawon Kim,* Heedoo Lee,* Scott R. Manson,[†] Maria Lindahl,[‡] Bradley Evans,[§] Jeffrey H. Miner,^{**} Fumihiko Urano,^{†**} and Ying Maggie Chen*

*Division of Nephrology, Department of Internal Medicine, [†]Division of Urology, Department of Surgery, Departments of [‡]Cell Biology and Physiology and ^{**}Pathology and Immunology, and [§]Division of Endocrinology, Metabolism and Lipid Research, Department of Internal Medicine, Washington University School of Medicine, St. Louis, Missouri; [‡]Institute of Biotechnology, University of Helsinki, Helsinki, Finland; and [§]Proteomics and Mass Spectrometry Facility, Donald Danforth Plant Science Center, St. Louis, Missouri

ABSTRACT

Endoplasmic reticulum (ER) stress and disrupted proteostasis contribute to the pathogenesis of a variety of glomerular and tubular diseases. Thus, it is imperative to develop noninvasive biomarkers for detecting ER stress in podocytes or tubular cells in the incipient stage of disease, when a kidney biopsy is not yet clinically indicated. Mesencephalic astrocyte–derived neurotrophic factor (MANF) localizes to the ER lumen and is secreted in response to ER stress in several cell types. Here, using mouse models of human nephrotic syndrome caused by mutant laminin $\beta 2$ protein–induced podocyte ER stress and AKI triggered by tunicamycin– or ischemia–reperfusion–induced tubular ER stress, we examined MANF as a potential urine biomarker for detecting ER stress in podocytes or renal tubular cells. ER stress upregulated MANF expression in podocytes and tubular cells. Notably, urinary MANF excretion concurrent with podocyte or tubular cell ER stress preceded clinical or histologic manifestations of the corresponding disease. Thus, MANF can potentially serve as a urine diagnostic or prognostic biomarker in ER stress–related kidney diseases to help stratify disease risk, predict disease progression, monitor treatment response, and identify subgroups of patients who can be treated with ER stress modulators in a highly targeted manner.

J Am Soc Nephrol 27: 2974–2982, 2016. doi: 10.1681/ASN.2014100986

Emerging evidence has shown that endoplasmic reticulum (ER) stress or the derangement of ER proteostasis contributes to the development and progression of glomerular and tubular diseases.¹ The ER is the central site for folding, post-translational modifications, and transport of secretory and membrane proteins. Environmental and genetic factors disrupting ER function lead to accumulation of misfolded and unfolded proteins in the ER lumen, which is termed ER stress.² Sustained or intense ER stress and

dysregulation of the unfolded protein response pathway ultimately lead to cell death.³

FSGS is the most common primary glomerular disorder leading to ESRD. Seminal advances in human genetics have identified FSGS as a primary podocytopathy, with major discoveries of podocyte–specific gene mutations.⁴ Mutations can lead to protein misfolding and disruption of protein trafficking.^{5,6} It has been shown that congenital nephrotic syndrome (NS) and familial

FSGS with mutations in podocyte genes, including *nephrin* (*NPHS1*), *podocin* (*NPHS2*), and α -*actinin-4* (*ACTN4*), are associated with accumulation of mutated proteins and ER stress *in vitro* and *in vivo*.^{7–9} Recently, we showed that the C321R mutation of the glomerular basement membrane (GBM) constituent laminin $\beta 2$ (*LAMB2*) leads to podocyte ER stress and defective secretion of laminin from podocytes to the GBM because of $\beta 2$ -protein misfolding, resulting in NS and human Pierson syndrome.^{10,11} In addition, a recent study showed that podocyte ER stress arising from a mutant *COL4A3* chain contributes to the pathogenesis of Alport syndrome.¹² In renal tubular cells, dysregulation of the unfolded protein response pathway induces injury and apoptosis.^{13–17} Thus, discovering an ER stress biomarker will enable identification of subjects with a

Received October 10, 2014. Accepted January 15, 2016.

Published online ahead of print. Publication date available at www.jasn.org.

Correspondence: Dr. Ying Maggie Chen, Washington University School of Medicine, Division of Nephrology, Campus Box 8126, 660 South Euclid Avenue, St. Louis, MO 63110. Email: ychen@dom.wustl.edu

Copyright © 2016 by the American Society of Nephrology

high risk of disease progression. In addition, early detection and intervention aimed at alleviating ER stress and restoring ER homeostasis may well be less challenging than reversing established kidney cell injury. However, there are no known podocyte or renal tubular cell ER stress biomarkers to date.

Here, for the first time, we show that mesencephalic astrocyte-derived neurotrophic factor (MANF) can serve as a potential urine biomarker for ER stress-associated kidney diseases.

MANF, a recently identified 18-kD highly soluble protein localized to the ER lumen, lacks the ER retention sequence (KDEL) at its carboxyl terminus in contrast to many other ER-resident endoplasmic reticulum stress response (ERSR) proteins.^{18,19} MANF is induced and secreted in response to experimental ER stress in several cell populations *in vitro*¹⁸ and *in vivo*.²⁰ However, this protein has not been studied in renal disease contexts.

We investigated whether MANF was induced in ER-stressed podocytes by using a podocyte ER stress-induced NS model that we have developed (Figure 1A).¹⁰ We have previously shown that, in *Lamb2*^{-/-};nephlin promoter (NEPH)-transgenic wild-type (Tg-WT) mice, expression of the WT rat LAMB2 cDNA in podocytes *via* the podocyte-specific mouse NEPH is sufficient to restore the integrity of the glomerular filtration barrier in *Lamb2*^{-/-} mice.²¹ We have also shown that *Lamb2*^{-/-} mice expressing the C321R rat LAMB2 in podocytes (*Lamb2*^{-/-};NEPH-C321R-LAMB2 mice) recapitulate features of patients with NS carrying the C321R-LAMB2 mutation.¹⁰ The high C321R transgene expressers on the *Lamb2*^{-/-} background (Tg-C321R mutants) exhibit LAMB2 transcript levels in podocytes comparable with those in the Tg-WT mice, albeit a much lower level of β 2-protein accumulation in the GBM.¹⁰ In the first postnatal month, when Tg-C321R mutants exhibit trace proteinuria without notable renal histologic alternations, podocyte ER stress induced by the C321R misfolded protein is evident.¹⁰ In this study, as shown by

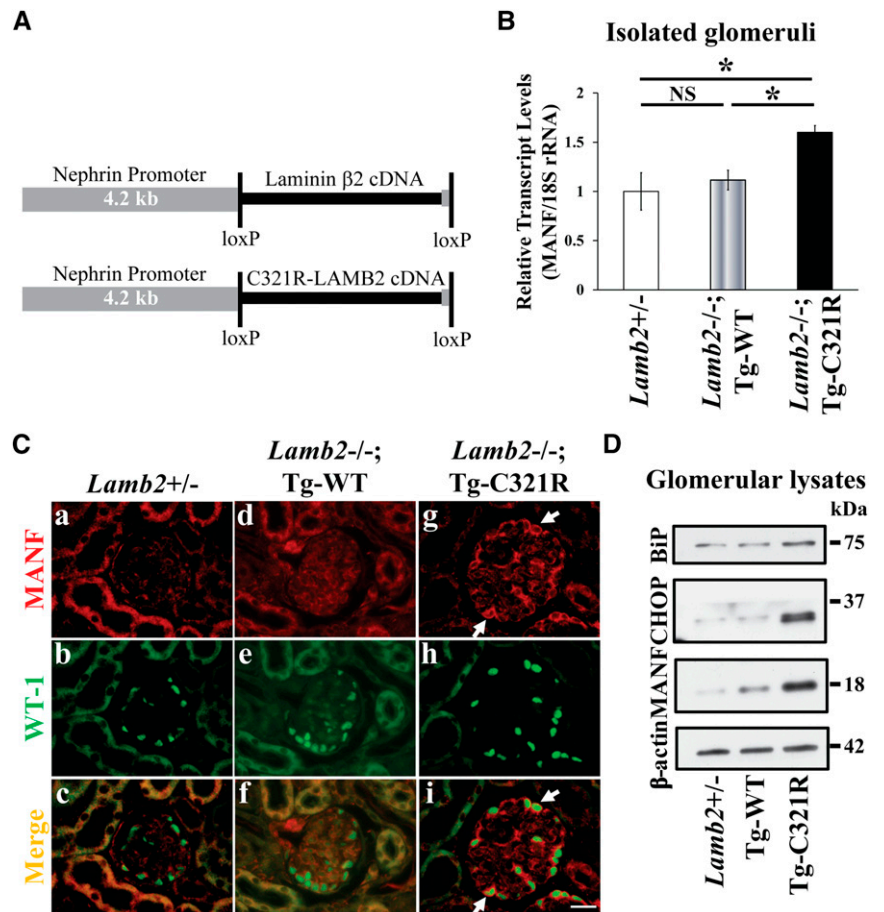


Figure 1. MANF is induced in ER-stressed podocytes in *Lamb2*^{-/-};NEPH-C321R-LAMB2 mice at an early stage of disease. (A) Schematic representation of the transgenes. The NEPH-B2 and NEPH-C321R-LAMB2 transgenes drive WT or C321R mutant- β 2 expression, respectively, from the podocyte-specific mouse NEPH. The β 2-cDNA sequences are flanked by loxP sites for future manipulations.^{10,21} (B) Quantitative real-time PCR analysis of MANF mRNA in isolated glomeruli from *Lamb2*^{+/-}, *Lamb2*^{-/-};Tg-WT, and *Lamb2*^{-/-};Tg-C321R mice at P24. MANF expression was normalized as a ratio to mouse 18S rRNA, and the average MANF-to-18S rRNA ratio in *Lamb2*^{+/-} mice was set as one ($n=3-4$ mice per genotype; mean \pm SD). * $P<0.05$; NS: not significant by ANOVA with Tukey multiple comparison test. (C) Paraffin kidney sections from mice of the indicated genotypes were examined by (c, f, and i) dual immunofluorescence staining (merge) of (a, d, and g) MANF (red) and (b, e, and h) WT-1 (green) at P25. Arrows indicate MANF staining in the podocytes of Tg-C321R glomeruli. Scale bar, 20 μ m. (D) Isolated glomerular lysates from *Lamb2*^{+/-}, *Lamb2*^{-/-};Tg-WT, and *Lamb2*^{-/-};Tg-C321R mice at P25 were analyzed by WB for levels of BiP, CHOP, MANF, and β -actin. The WB image shown is representative of at least three independent experiments.

double-immunofluorescence staining of MANF and the podocyte nucleus marker WT-1, Tg-C321R podocytes exhibited MANF upregulation in almost all glomeruli at P25 (Figure 1, C, g-i) compared with levels in podocytes of WT (Figure 1, C, a-c) and *Lamb2*^{-/-};Tg-WT (Figure 1, C, d-f) mice. Western blot (WB) analysis confirmed that expression of MANF

along with other important ER stress markers, including Ig binding protein (BiP) and C/EBP homologous protein (CHOP), an ER stress-specific proapoptotic transcription factor, was increased in Tg-C321R glomeruli versus the WT and Tg-WT glomeruli (Figure 1D) at P25. Meanwhile, MANF transcript levels were significantly increased in Tg-C321R

glomeruli compared with the WT and Tg-WT glomeruli at P24 (Figure 1B). Collectively, these data show that MANF is induced in ER-stressed podocytes in the incipient stage of proteinuria in our NS animal model.

To define MANF induction at the subcellular level and whether MANF was secreted in response to ER stress triggered by the C321R mutation, our cell model harboring the C321R-LAMB2 mutation, which is located in the LEa domain of $\beta 2$, was used. In stably transfected human embryonic kidney 293T cells expressing *Gaussia* luciferase (Gluc) –tagged WT or mutant $\beta 2$ -amino-terminal and adjacent LEa domains, we have shown previously that the misfolded C321R protein upregulates expression of BiP.¹⁰ In agreement with the *in vivo* data, the C321R/Gluc fusion protein significantly increased MANF expression at both transcriptional (Figure 2C) and translational (Figure 2A) levels compared with the WT/Gluc fusion protein. Treatments with tunicamycin (TM), which blocks N-linked glycosylation in the ER and triggers ER stress, were included as positive controls (Figure 2A). Moreover, confocal immunofluorescence microscopy revealed that the induced MANF in C321R cells (Figure 2, B, d) overlapped exclusively with ER-targeted green fluorescent protein (GFP) (Figure 2, B, d–f). More interestingly, a higher level of MANF was detected in concentrated conditioned medium from the C321R cells compared with the WT cells (Figure 2D), corresponding to the MANF induction in the serum-starved C321R cells versus WT cells (Figure 2D). To determine whether MANF was also secreted from ER-stressed podocytes, primary podocytes were isolated and cultured from *Lamb2*^{+/-}, *Lamb2*^{-/-};Tg-C321R, and *Lamb2*^{-/-};Tg-WT mice at P25. Real-time PCR showed that the C321R mutation increased MANF mRNA expression (Figure 2G). Most importantly, as shown in Figure 2F, secretion of MANF by Tg-C321R podocytes was easily detected in unconcentrated medium and significantly higher compared with that by WT and Tg-WT podocytes,

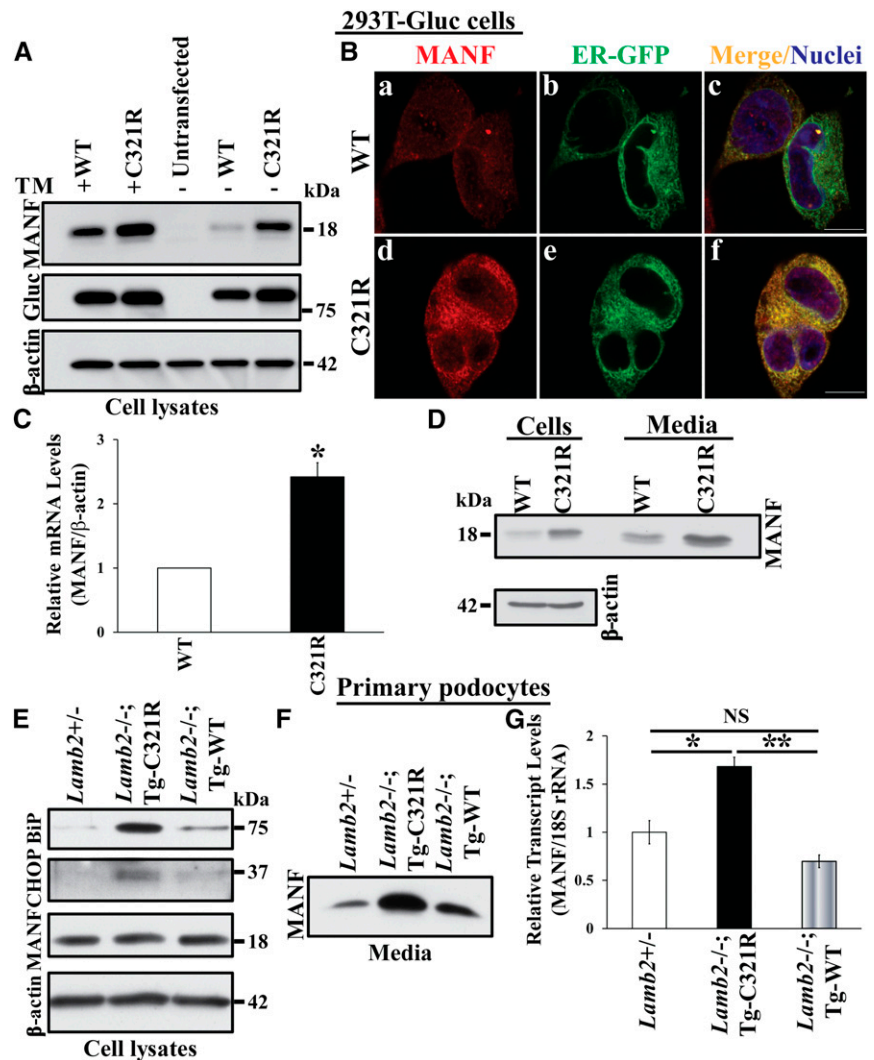


Figure 2. The C321R-LAMB2 mutation induces MANF expression and secretion *in vitro*. The results in A–D and E–G were derived from stably transfected 293T-Gluc cells and cultured primary podocytes of the indicated genotypes, respectively. (A) Cell lysates from untransfected 293T cells or stable 293T transfectants expressing either the WT/Gluc or the C321R/Gluc fusion protein were analyzed by WB with the indicated antibodies. TM-treated cells served as positive controls. (B) Accumulation of MANF in the ER of the C321R mutant cells. 293T-Gluc cells were transduced with (b and e) CellLight ER-GFP (green), an inactivated baculovirus expressing GFP fused to an ER signal sequence and KDEL. The cells were then stained with (a and d) an anti-MANF antibody (red). Nuclei were counterstained with (c and f) Hoechst 33342 (blue), and confocal images were acquired. Scale bars, 10 μ m. (C) Quantitative RT-PCR for MANF mRNA in WT/Gluc and C321R/Gluc cells. Mean \pm SD of fold changes of three independent samples from each clone. * $P < 0.05$ versus WT control by *t* test. (D) Immunoblot analysis for MANF secretion into the conditioned media of serum-starved WT and C321R mutant cells. Stably transfected 293T-Gluc cells at 60%–80% confluence were serum starved for 37 hours. The conditioned media were harvested, concentrated, and subjected to WB together with the serum-starved cell lysates. (E) Primary podocyte cell lysates from age-matched *Lamb2*^{+/-}, *Lamb2*^{-/-};Tg-C321R, and *Lamb2*^{-/-};Tg-WT mice at P25 were analyzed by WB with the indicated antibodies. (F) Immunoblot analysis for MANF secretion into the media by primary podocytes from the indicated genotypes at P25. MANF secretion into the media was normalized to the corresponding cellular protein amount. (G) Quantitative real-time PCR analysis of MANF mRNA in primary podocytes from *Lamb2*^{+/-}, *Lamb2*^{-/-};Tg-C321R, and *Lamb2*^{-/-};Tg-WT mice at P25. MANF expression was normalized as a ratio to mouse 18S rRNA, and the

analogous to the analysis of urinary MANF excretion as shown below. MANF secretion by primary podocytes was so rapid that no difference of MANF expression in the podocyte cell lysates was observed among different genotypes, although Tg-C321R podocytes indeed underwent ER stress as shown by induction of BiP and CHOP (Figure 2E). Taken together, these results indicate that MANF is an ER stress–dependent and secreted ERSR protein responding to the effects of the C321R-LAMB2 mutant protein.

Next, we determined whether MANF was upregulated in renal tubular cells under ER stress. Intraperitoneal injection of TM results in AKI characterized by proximal tubular cell damage peaking between 4 and 5 days after injection because of activation of CHOP and subsequent apoptosis of renal tubular cells.²² Whereas profound cortical tubular necrosis, as manifested by tubular dilation and loss of brush borders, was observed in kidneys 5 days after 1 mg/kg TM injection (Figure 3, A, g and h), no obvious renal histopathologic changes (Figure 3, A, d and e) or significant upregulation of kidney injury molecule-1, an early kidney injury marker, were observed after 24 hours (Supplemental Figure 1, E–H). The glomeruli were spared during disease progression (Figure 3, A, c, f, and i). Correlating with renal morphologic changes, BUN levels were elevated on day 5 but not at 24 hours (Figure 3B). In contrast, analysis of *ERSR* gene expression showed significant upregulation of MANF mRNA along with BiP, CHOP, and ER degradation–enhancing α -mannosidase–like protein 24 hours after TM injection versus day 5 after injection or controls (Figure 3C). Furthermore, MANF protein expression in kidneys was higher at 24 hours compared with day 5 postinjection or controls (Figure 3, D and E). Dual immunostaining for MANF and the proximal tubular marker *Lotus tetragonolobus* lectin (LTL)

showed that MANF induction at 24 hours after TM treatment occurred predominantly in the proximal tubules but not in other tubular segments (Figure 3, F, e–g) or glomeruli (Figure 3, F, d, h, and l). Double immunostaining of MANF with ER stress markers protein disulfide isomerase A3 (PDIA3) and CHOP confirmed that induction of MANF coincided with upregulation of these ERSR proteins in renal tubules at 24 hours after TM injection (Supplemental Figure 2). Together, these results directly show that MANF is upregulated in ER–stressed proximal tubular cells and precedes histologic and renal functional changes in this TM–induced AKI mouse model.

We further investigated whether MANF was induced in tubular cells in other forms of AKI with tubular ER stress. AKI secondary to ischemia-reperfusion (I/R) is a common and potentially devastating clinical problem. The current treatment for AKI is mainly supportive because of a paucity of early mechanistic biomarkers. Growing evidence has shown that ER stress plays an important role linking ischemic insult and injury in renal tubules.^{23,24} In an established mouse I/R model, acute tubular necrosis was predominantly observed in the corticomedullary junction area at 9 hours after reperfusion after bilateral renal ischemia for 30 minutes (Supplemental Figure 3, A, c and d). Although serum creatinine levels in the I/R-injured mice were increased compared with those in sham-operated mice, the elevation did not achieve statistical significance (Supplemental Figure 3B). Meanwhile, *ERSR* genes, including *BiP*, *CHOP*, and *MANF*, were upregulated at transcriptional and translational levels (Supplemental Figure 3, C and D). Coimmunostaining of kidney sections for MANF and LTL showed that MANF induction occurred in injured proximal tubular cells (Supplemental Figure 3E).

Finally, we sought to determine whether MANF from ER-stressed podocytes or tubular cells was released into the urine and hence, could be detected in urine at an early stage of the disease. Indeed, MANF immunoreactivity (Abnova, Walnut, CA) was easily detected in urine specimens from TM-injected mice within 24 hours (Figure 4A), I/R-injured mice within 6 hours of reflow (Supplemental Figure 3F), and C321R mutants at the incipient stage of NS (Figure 4D) but not in the controls. Urinary MANF excretion in TM-injected mice was not dependent on albuminuria, which was not present (Figure 4C). The prominent immunoreactive MANF band consistently migrated at approximately 37 kD in urine samples from mice with tubular ER stress (Figure 4A, arrow, Supplemental Figure 3F) and approximately 30 kD from Tg-C321R mutants with podocyte ER stress at the early stage of proteinuria (Figure 4D), whereas the band at the expected position of MANF (Figure 4A, arrowhead) was not always detectable. The same pattern of MANF immunoreactivity in urine was observed with another anti-MANF antibody (Proteintech, Chicago, IL) recognizing different epitopes (Supplemental Figure 4, A and B). In addition, a peptide competition assay, an accepted method to confirm the specificity of an antibody to its immunogen, showed that preincubating the anti-MANF antibody with its immunizing peptide, which does not share homology with any other proteins except MANF, completely abolished binding to the approximately 37-kD (Supplemental Figure 4C) and approximately 30-kD bands (Supplemental Figure 4D). To definitively prove that the approximately 37-kD band in urine from AKI mice contains MANF, *Manf*^{−/−} mice²⁵ and WT littermates were injected with TM (1 mg/kg) or vehicle control. MANF ablation completely eliminated both the approximately 18-kD and

average MANF-to-18S rRNA ratio in *Lamb2*^{+/-} mice was set as one ($n=4$ mice per genotype; mean \pm SD). * $P<0.05$; ** $P<0.001$; NS: not significant by ANOVA with Tukey multiple comparison test. All WB images are representative of at least three independent experiments.

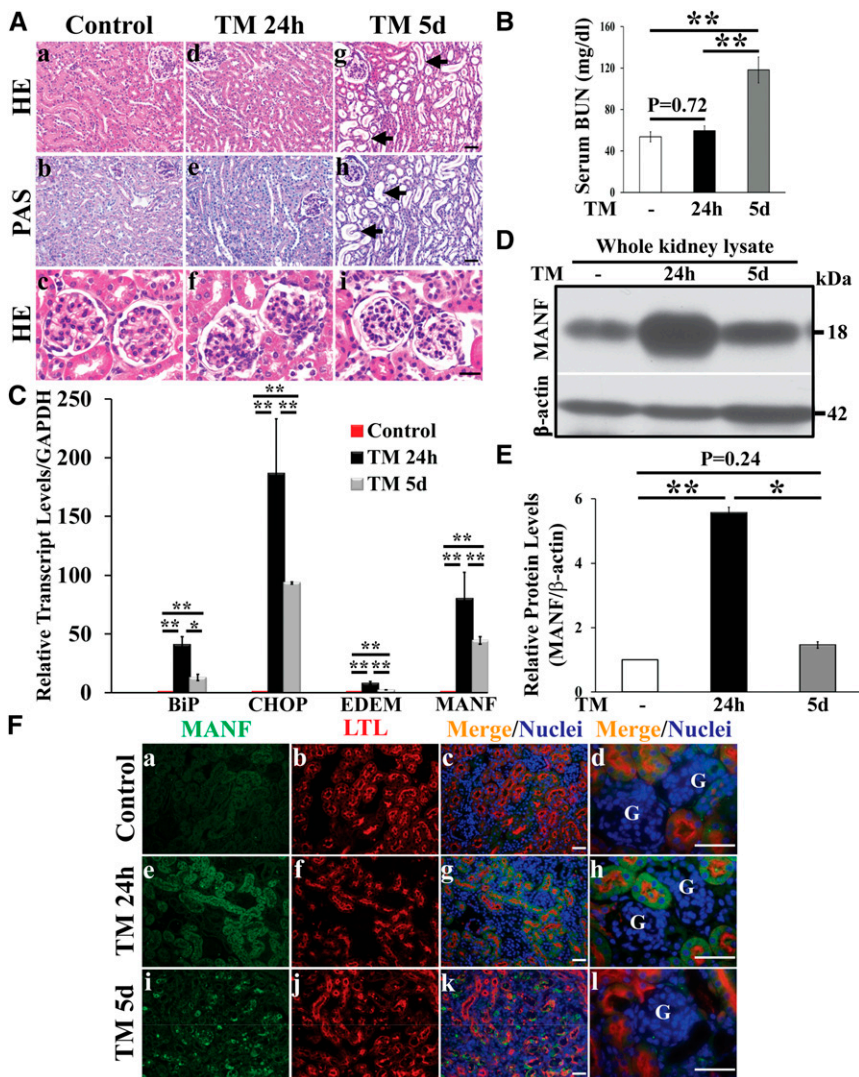


Figure 3. MANF upregulation in ER-stressed renal tubular cells precedes the histologic changes and decline of renal function in a mouse model of TM-induced AKI. (A) Hematoxylin and eosin (HE) and periodic acid-Schiff (PAS) staining of paraffin kidney sections from (a–c) control (DMSO vehicle injected) and (d–i) TM-injected (1 mg/kg intraperitoneally) mice: (d–f) 24 hours after TM injection and (g–i) 5 days after injection ($n=5$ mice per group). Note the presence of extensive tubular dilation, epithelial flattening, tubular basement membrane denudation, and loss of brush borders in the proximal tubules (arrows in g and h) on day 5 and the absence of conspicuous light microscopic changes on day 1 after TM injection. Scale bars, 40 μ m. (B) BUN levels for the indicated groups: controls ($n=7$), 24 hours after treatment with TM (1 mg/kg; $n=8$), and 5 days after treatment with TM ($n=4$; mean \pm SD). $^{**}P<0.001$ by ANOVA with Tukey multiple comparison test. (C) Quantitative RT-PCR showed relative transcript levels of *ERSR* genes, including *BiP*, *CHOP*, *endoplasmic reticulum degradation-enhancing α -mannosidase-like (EDEM)*, and *MANF*, in kidneys at the indicated time points after TM injection (1 mg/kg) compared with controls. Absolute levels were normalized first to those of GAPDH and then, to the levels in the control kidneys (mean \pm SD). $^{*}P<0.05$ by ANOVA with Tukey multiple comparison test ($n=5$ mice per group); $^{**}P<0.001$ by ANOVA with Tukey multiple comparison test ($n=5$ mice per group). (D) Whole-kidney lysates from mice treated with or without TM (1 mg/kg) at different time points were analyzed by WB for levels of MANF and β -actin. (E) Quantification of MANF normalized to β -actin in kidney lysates in three independent experiments. The average MANF-to- β -actin ratio in vehicle-treated mice was set as one (mean \pm SD). $^{*}P<0.05$ by ANOVA with Tukey multiple comparison test; $^{**}P<0.001$ by ANOVA with

approximately 37-kD bands in the urine (Figure 4B). To confirm that the approximately 30-kD band in urine from mice with ER-stressed podocytes comprises MANF, a liquid chromatography-tandem mass spectrometry (LC-MS/MS) analysis was performed on the designated band in gel (Supplemental Figure 5B) after enrichment of urinary MANF by immunoprecipitation (Supplemental Figure 5A). Mass spectrometry analysis identified MANF in the approximately 30-kD band from the urine of the C321R mutant mice (Supplemental Figure 5C, Supplemental Table 1). Together, these data confirm the specificity of the anti-MANF antibodies and show that the upper bands (approximately 30 kD and approximately 37 kD) contain MANF. The reasons for the different sizes in urine observed by WB are currently unknown but could result from different post-translational modifications or either dimerization or crosslinking to another protein in the urinary milieu, which is characterized by high concentrations of sodium ion and urea and high osmolality at the tip of the loop of Henle. The exact mechanism responsible for the formation of the upshifted bands in the urine warrants additional investigation. Interestingly, urinary MANF excretion increased during disease progression in the nephrotic C321R mutants, with the approximately 18-kD band becoming more evident (Figure 4E). This most likely reflects increased podocyte ER stress, paralleling the accumulated misfolded β 2 protein at 6 or 8 weeks of age. These results show that urinary MANF excretion coincides with podocyte or tubular cell ER stress and precedes clinical or histologic changes of the corresponding disease.

In conclusion, our study has identified MANF as a mechanistic urine biomarker for detecting ER stress in podocytes or renal tubular cells in mice noninvasively and early in disease development. We will continue to validate this novel urine biomarker in human kidney diseases associated with ER stress. Extensive potential clinical applications can be envisioned as follows. (1) Hereditary

proteinuric diseases, including congenital NS, familial FSGS, and Alport syndrome, caused by various podocyte gene mutations. Increasingly more pathogenic genetic variants in podocyte genes that may induce podocyte ER stress will be identified with the recent advent of next generation sequencing. (2) Diverse sporadic nephropathies, including FSGS, membranous nephropathy, minimal change disease, and diabetic nephropathy. Multiple studies have linked podocyte ER stress to the pathogenesis of these diseases in both experimental models^{26–28} and human kidney biopsies.^{29,30} (3) AKI resulting from tubular ER stress (for example, in the setting of ischemia injury and hyperglycemia^{13,16,17}). On the basis of our mouse studies, MANF can potentially serve as a urine biomarker for early diagnosis, prediction of disease progression, and treatment response monitoring in these podocyte ER stress- or renal tubular ER stress-related kidney diseases. MANF can also help identify subgroups of patients with ER dysfunction who can be treated with ER stress modulators in a highly targeted manner.

CONCISE METHODS

Mice and Treatment with TM

The *Lamb2* null, WT, and mutant Tg mice and *Manf* null mice have all been described previously.^{10,21,25} TM was purchased from Sigma-Aldrich (St. Louis, MO), dissolved in DMSO at 2 mg/ml, and injected intraperitoneally at 1 mg/kg into 6- to 10-week-old C57BL/6J mice (stock no. 000664; The Jackson Laboratory, Bar Harbor, ME) and 8-week-old *Manf* null and WT littermates. All animal experiments conformed to the National Institutes of Health (NIH) Guide for the Care and Use of Laboratory Animals and were approved by the Washington University Animal Studies Committee. TM injection experiments conducted on *Manf*^{-/-} mice and WT littermates in Finland were approved by the National Animal

Experiment Board in Finland (animal license no. ESAVI/8189/04.10.07/2015).

Establishment of Stable 293T Cells Expressing Gluc-Tagged LAMB2 Fragments

The stably transfected 293T-Gluc cells carrying WT and site-directed mutant rat LAMB2 fragments containing the β 2-amino-terminal and LEa domains were generated, and individual clones were selected as previously described.¹⁰ Established clones were maintained in DMEM (Gibco, Grand Island, NY) supplemented with 10% heat-inactivated FBS (Gibco) and 25 μ g/ml Zeocin.

Isolation of Mouse Glomeruli

Mice were perfused through the heart with magnetic 4.5- μ m-diameter Dynabeads (Dynabeads M-450 Tosylactivated; Invitrogen, Carlsbad, CA). Kidneys were minced into small pieces, digested by collagenase A (Gibco) and DNase I (Sigma-Aldrich), filtered, and collected using a magnet. The purity of glomeruli was >95%. The isolated glomeruli retained intact mRNA integrity as confirmed by RNA electropherogram.

Primary Podocyte Culture

Isolated glomeruli from *Lamb2*^{+/-}, *Lamb2*^{-/-}; Tg-C321R, and *Lamb2*^{-/-};Tg-WT mice at P25 were suspended in DMEM:Ham F-12 (2:1) that contained 0.45 μ m filtered 3T3-L1 supernatant, 5% heat-inactivated FBS, Insulin-Transferrin-Sodium Selenite liquid media supplement, and 100 U/ml penicillin-streptomycin; plated onto collagen type 1-coated petri dishes; and incubated at 37°C in room air with 5% CO₂. After 3 days, cell colonies began to sprout around the glomeruli. These cells (P0) showed an epithelial morphology with a polyhedral shape when confluence was reached and were characterized as podocytes by detection of the podocyte-specific markers, WT-1 and nephrin, by immunofluorescence staining. Only passages 1 and 2 podocytes from the indicated genotypes were used in the *in vitro* studies.

Antibodies and Reagents

Commercially available antibodies were obtained as follows: rabbit anti-mouse MANF antibodies were from Abnova and Proteintech, goat anti-mouse MANF antibody was from Santa Cruz Biotechnology (Santa Cruz, CA), mouse IgG1 anti-mouse WT-1 and mouse IgG2b anti-mouse CHOP (9C8) antibodies were from Thermo Scientific (Kalamazoo, MI), goat anti-mouse nephrin antibody was from R&D Systems (Minneapolis, MN), and horseradish peroxidase (HRP)-conjugated anti-mouse β -actin antibody crossreacting with human was from Sigma-Aldrich. Alexa 488- and Alexa 594-conjugated secondary antibodies were purchased from Molecular Probes (Carlsbad, CA). HRP-conjugated anti-rabbit secondary antibody was from Santa Cruz Biotechnology. Biotinylated LTL and anti-rabbit antibody were from Vector Laboratories (Burlingame, CA). CellLight ER-GFP *BacMam 2.0* and Alexa 594-conjugated streptavidin were purchased from Molecular Probes. Rat collagen 1 was from Trevigen (Gaithersburg, MD). Recombinant mouse MANF with a carboxyl-terminal polyhistidine tag was obtained from Sino Biologic Inc. (Beijing, China).

Immunofluorescence Staining and Confocal Microscopy

Immunofluorescence staining on paraffin sections was performed as described previously.¹⁰ For MANF staining in glomeruli, kidneys were fixed by transcardiac perfusion with 4% paraformaldehyde in PBS, and paraffin-embedded sections were used. After dewaxing, the antigen was retrieved by Retrieval Solution A Working Solution (BD Pharmingen, San Jose, CA) for 10 minutes at 89°C. Nonspecific avidin binding was blocked by an Avidin/Biotin Blocking Kit (Vector Laboratories) before incubating kidney sections with 1% BSA for 30 minutes at room temperature. The slides were incubated with rabbit anti-mouse MANF together with mouse IgG1 anti-mouse WT-1 antibodies. A biotinylated anti-rabbit antibody was used to amplify fluorescence signals for MANF followed by Alexa 594-conjugated streptavidin and an

Tukey multiple comparison test. (F) Double-immunofluorescence staining for (a, e, and i) MANF (green) and (b, f, and j) LTL (red) on paraffin kidney sections from mice treated with vehicle or TM (1 mg/kg) at the indicated time points. Nuclei were counterstained with (c, d, g, h, k, and l) Hoechst 33342 (blue). G, glomerulus. Scale bars, 40 μ m.

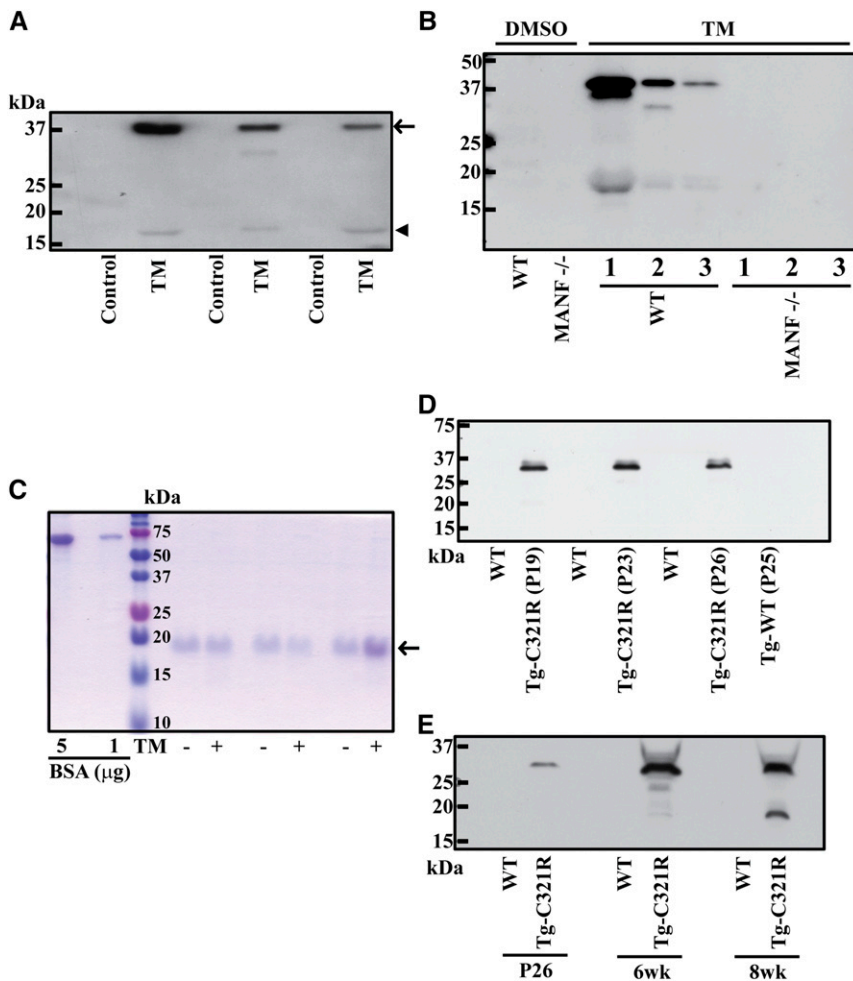


Figure 4. MANF is an ER stress–dependent molecular marker in urine. (A) Detection of urinary MANF within 24 hours of TM injection. Urines were collected for 24 hours after the mice were injected with vehicle or 1 mg/kg TM intraperitoneally. Crude urine samples from mice treated with vehicle ($n=12$) or TM ($n=16$) were analyzed by WB (Abnova) for MANF excretion. The arrowhead marks the expected position of MANF (approximately 18 kD), and the upper band marked by the arrow (approximately 37 kD) showed intense MANF immunoreactivity. (B) Urine specimens from *Manf*^{+/+} and *Manf*^{-/-} mice (8 weeks of age; nine mice per genotype) injected with vehicle (DMSO) or TM (1 mg/kg intraperitoneally) were assayed for MANF by WB. The urines were collected within 24 hours of TM injection. (C) The same urine samples in A were analyzed by SDS-PAGE (1 μ l per lane) and stained with Coomassie Blue. BSA was used as a positive control. The arrow marks nonspecific tubular proteins on the gel. (D) Urinary MANF excretion was assessed by WB from *Lamb2*^{-/-};NEPH-C321R-LAMB2 mice and their *Lamb2*^{+/+} littermates and age–matched *Lamb2*^{-/-};NEPH-Tg-WT mice ($n=10$, $n=10$, and $n=4$, respectively). Shown is one representative experiment at the indicated ages. (E) Immunoblot analysis of MANF in crude urine specimens from one pair of *Lamb2*^{+/+} and *Lamb2*^{-/-};Tg-C321R littermates following the disease course. Shown is one representative experiment. Two more independent experiments were performed with similar results. The urinary MANF excretion was normalized to urine creatinine excretion, such that the urine volume applied to the gel reflected the amount of urine containing 3 μ g creatinine for A, 1.5 μ g creatinine for B, 2 μ g creatinine for D, and 1 μ g creatinine for E.

Alexa 488–conjugated anti–mouse secondary antibody. For dual staining of MANF with biotinylated LTL, MANF signals were not

amplified by using the biotin/avidin system. Slides were analyzed under a fluorescence microscope (Nikon, Tokyo, Japan).

For immunocytochemistry, 293T-Gluc cells were seeded on coverslips coated with 5 μ g/ml rat collagen 1 that was dissolved in 0.02 M acetic acid on 24-well plates for 48 hours. After overnight transduction with CellLight ER-GFP, the cells were fixed with 4% paraformaldehyde for 20 minutes, permeabilized with 1% Triton X-100 for 5 minutes at room temperature, and blocked with 1% BSA for 30 minutes at room temperature followed by incubation with the rabbit anti–MANF antibody (Abnova) overnight. The coverslips were washed with PBS and incubated with the Alexa 594–conjugated anti–rabbit antibody and Hoechst 33342 to stain nuclei. The coverslips were then mounted with anti-quench solution and visualized using Nikon TE-2000 Confocal Microscopy.

Light Microscopy

For light microscopy, kidneys were fixed in 4% paraformaldehyde, dehydrated through graded ethanols, embedded in paraffin, sectioned at 4 μ m, and stained with hematoxylin and eosin and periodic acid–Schiff by standard methods.

WB Analyses

Stable 293T-Gluc cells, isolated glomeruli, and primary podocytes were lysed by RIPA buffer (Sigma-Aldrich) containing protease inhibitor cocktail (Roche Diagnostics, Indianapolis, IN). TM-untreated and -treated kidneys were extracted using the same lysis buffer with the protease inhibitors and homogenized by sonication. The protein concentrations of cell and kidney lysates were determined by Bio-Rad Protein Assay (Bio-Rad, Hercules, CA) using BSA as a standard. Denatured proteins were separated on SDS-PAGE and then, transferred to polyvinylidene difluoride membranes. Blots were blocked with 5% nonfat milk for 1 hour and then, incubated overnight with primary antibodies. The membranes were washed with Tris-buffered saline/Tween buffer and incubated with the appropriate HRP–conjugated secondary antibodies. The proteins were then visualized in an x-ray developer using ECLplus Detection Reagents (GE Healthcare, Waukesha, WI). To ensure equal protein loading, the same blot was stripped with stripping buffer (25 mM glycine and 1% SDS, pH 2.0) and then incubated with an HRP–conjugated mouse anti–human (and mouse) β -actin

antibody. Relative intensities of protein bands were quantified using ImageJ (NIH) analysis software.

To examine secretion of MANF protein in conditioned cell medium, equal numbers of 293T-Gluc cells expressing either the WT/Gluc or the C321R/Gluc fusion protein at 60%–80% confluence were changed to serum-free media. Thirty-seven hours later, conditioned media were harvested and clarified by centrifugation at 500 rpm for 5 minutes; 3.9 ml conditioned medium was concentrated using Amicon Ultra 4 ml (EMD Millipore, Billerica, MA) before being subjected to WB analysis. To determine secretion of MANF from primary podocytes, equal numbers of primary podocytes from the indicated genotypes were plated, and their media were harvested after 48 hours of culturing before subjecting them to the WB analysis. The MANF secretion was further normalized to corresponding cellular protein amount because of significantly slower growth rate of Tg-C321R podocytes compared with that of control podocytes. To compare urinary MANF excretion, crude urine samples from the indicated groups that were normalized to creatinine were applied to a gel.

mRNA Quantification by Real-Time PCR

Total RNA from isolated glomeruli, whole kidneys, the individual WT and mutant 293T-Gluc clones, or primary podocytes was extracted using the RNeasy Kit (Qiagen, Germantown, MD) with subsequent DNase I treatment. 0.5 μ g glomerular RNA or 1 μ g kidney and cellular RNA was then reverse transcribed using an RT-PCR Kit (Superscript III; Invitrogen). Gene expression was evaluated by quantitative real-time PCR; 1 μ l cDNA was added to SYBR Green PCR Master Mix (Qiagen) and subjected to PCR amplification (one cycle at 95°C for 20 seconds and 40 cycles at 95°C for 1 second and 60°C for 20 seconds) in an Applied Biosystems 7900HT Fast Real-Time PCR System (Life Technologies, Grand Island, NY) using mouse 18S rRNA or GAPDH or human β -actin as an internal control. Quantitative PCR was conducted in triplicate for each sample. The sequences of primers were mouse MANF forward: TCTGGGACGATTTAC-CAGGA and reverse: CTTGCTTCACGG-CAAACTTT; human MANF forward:

CGGTTGTGCTACTATATCGGGG and reverse: GGCCAGAGGCTTTGATACCT; mouse BiP forward: TTCAGCCAATTATCAG-CAAACCTCT and reverse: TTTTCTGATG-TATCCTCTTCACCAGT; mouse CHOP forward: CCACCACACCTGAAAGCAGAA and reverse: AGGTGAAAGGCAGGGAC-TCA; mouse ER degradation-enhancing α -mannosidase-like protein forward: CT-ACCTGCGAAGAGGCCG and reverse: GTTCATGAGCTGCCACTGA; mouse 18S rRNA forward: GTAACCCGTTGA-ACCCCAT and reverse: CCATCCAATC-GGTAGTAGCG; mouse GAPDH forward: TGTAGACCATGTAGTTGAGGTCA and reverse: AGGTCGGTGTGAACGGATTTG; and human β -actin forward: GGCACC-CAGCACAATGAAG and reverse: GGC-ACCCAGCACAATGAAG.

BUN Measurement

BUN was measured by using a QuantiChrom Urea Assay Kit (DIUR-500; BioAssay Systems, Hayward, CA).

Urinalyses

Urine was collected from mice by manual restraint or using a metabolic cage if 24-hour urine collection was required, and it was centrifuged (1800 \times g for 10 minutes) to remove debris before processing for WB or albumin gel analyses. Equal volumes of urine (1 μ l) were run on precast 12.5% SDS polyacrylamide gels and stained with Coomassie Blue to visualize albumin. Urinary creatinine concentration was quantified by a QuantiChrom Creatinine Assay Kit (DICT-500; BioAssay Systems).

ACKNOWLEDGMENTS

We thank the Mouse Genetics Core, the Washington University Center for Kidney Disease Research (supported by National Institutes of Health [NIH] grant P30DK079333), and the Washington University Diabetes Research Center (supported by NIH grant P30DK020579) for generation of transgenic mice and collecting urine and the Musculoskeletal Research Center Morphology Core (supported by NIH grant P30AR057235) for histology. We also thank Petra Gilmore, Yiling Mi, and Rose Connors for expert technical assistance

and Dr. Reid Townsend for data analysis at the Washington University Proteomics Core for the Siteman Cancer Center (supported by the Washington University Institute of Clinical and Translational Sciences grant UL1 TR000448 from the National Center for Advancing Translational Sciences and National Institute of General Medical Sciences grant P41 GM103422-35). We thank Dr. Mike Naldrett for expert technical assistance and discussions at the Proteomics and Mass Spectrometry Facility at Donald Danforth Plant Science Center. We thank Tatiana Danilova and Emmi Pakarinen at the University of Helsinki for conducting tunicamycin injection experiments on *Manf*^{-/-} mice and wild-type littermates.

Mice were housed in a facility supported by NIH grant C06RR015502. J.H.M. was supported by NIH grants R01DK078314 and R56DK100593. F.U. was supported by NIH grants R01DK067493, R01DK016746, P30DK020579, and UL1TR000448; Juvenile Diabetes Research Foundation grants 47-2012-760 and 17-2013-512; American Diabetes Association grant 1-12-CT-61, the Samuel E. Schechter Professorship, the Ellie White Foundation for Rare Genetic Disorders, and the Jack and J.T. Snow Scientific Research Foundation. Y.M.C. was supported by NIH grants K08DK089015, R03DK106451, and P30DK079333 (Pilot and Feasibility Study); a Halpin Foundation–American Society of Nephrology Research grant; Faculty Scholar Award MD-FR-2013-336 from the Children's Discovery Institute of Washington University and St. Louis Children's Hospital; Clinical Scientist Development Award 2015100 from the Doris Duke Charitable Foundation; a Career Development Award from the Nephrotic Syndrome Study Network; and an Early Career Development Award from the Central Society for Clinical and Translational Research.

DISCLOSURES

A patent application entitled "Mesencephalic astrocyte-derived neurotrophic factor (MANF) as a urine biomarker for endoplasmic reticulum (ER) stress-related kidney disease, methods and uses therefore" has been filed by Y.M.C. and the Washington University Office of Technology Management (application no. 14730465; filed on June 4, 2015).

REFERENCES

1. Inagi R, Ishimoto Y, Nangaku M: Proteostasis in endoplasmic reticulum—new mechanisms in kidney disease. *Nat Rev Nephrol* 10: 369–378, 2014
2. Osowski CM, Urano F: Measuring ER stress and the unfolded protein response using mammalian tissue culture system. *Methods Enzymol* 490: 71–92, 2011
3. Ron D, Walter P: Signal integration in the endoplasmic reticulum unfolded protein response. *Nat Rev Mol Cell Biol* 8: 519–529, 2007
4. Grahammer F, Schell C, Huber TB: The podocyte slit diaphragm—from a thin grey line to a complex signalling hub. *Nat Rev Nephrol* 9: 587–598, 2013
5. Dobson CM: Protein misfolding, evolution and disease. *Trends Biochem Sci* 24: 329–332, 1999
6. Sanders CR, Nagy JK: Misfolding of membrane proteins in health and disease: The lady or the tiger? *Curr Opin Struct Biol* 10: 438–442, 2000
7. Cybulsky AV, Takano T, Papillon J, Bijian K, Guillemette J, Kennedy CR: Glomerular epithelial cell injury associated with mutant alpha-actinin-4. *Am J Physiol Renal Physiol* 297: F987–F995, 2009
8. Fan Q, Zhang H, Ding J, Liu S, Miao J, Xing Y, Yu Z, Guan N: R168H and V165X mutant podocin might induce different degrees of podocyte injury via different molecular mechanisms. *Genes Cells* 14: 1079–1090, 2009
9. Liu L, Doné SC, Khoshnoodi J, Bertorello A, Wartiovaara J, Berggren PO, Tryggvason K: Defective nephrin trafficking caused by missense mutations in the NPHS1 gene: Insight into the mechanisms of congenital nephrotic syndrome. *Hum Mol Genet* 10: 2637–2644, 2001
10. Chen YM, Zhou Y, Go G, Marmorstein JT, Kikkawa Y, Miner JH: Laminin β 2 gene missense mutation produces endoplasmic reticulum stress in podocytes. *J Am Soc Nephrol* 24: 1223–1233, 2013
11. Hasselbacher K, Wiggins RC, Matejas V, Hinkes BG, Mucha B, Hoskins BE, Ozaltin F, Nürnberg G, Becker C, Hangan D, Pohl M, Kuwertz-Bröking E, Griebel M, Schumacher V, Royer-Pokora B, Bakkaloglu A, Nürnberg P, Zenker M, Hildebrandt F: Recessive missense mutations in LAMB2 expand the clinical spectrum of LAMB2-associated disorders. *Kidney Int* 70: 1008–1012, 2006
12. Pieri M, Stefanou C, Zaravinos A, Erguler K, Stylianou K, Lapathitis G, Karaikos C, Savva I, Paraskeva R, Dweep H, Sticht C, Anastasiadou N, Zouvani I, Goumenos D, Felekis K, Saleem M, Voskarides K, Gretz N, Deltas C: Evidence for activation of the unfolded protein response in collagen IV nephropathies. *J Am Soc Nephrol* 25: 260–275, 2014
13. Bando Y, Tsukamoto Y, Katayama T, Ozawa K, Kitao Y, Hori O, Stern DM, Yamauchi A, Ogawa S: ORP150/HSP12A protects renal tubular epithelium from ischemia-induced cell death. *FASEB J* 18: 1401–1403, 2004
14. Kawakami T, Inagi R, Wada T, Tanaka T, Fujita T, Nangaku M: Indoxyl sulfate inhibits proliferation of human proximal tubular cells via endoplasmic reticulum stress. *Am J Physiol Renal Physiol* 299: F568–F576, 2010
15. Khan MA, Liu J, Kumar G, Skapek SX, Falck JR, Imig JD: Novel orally active epoxyeicosatrienoic acid (EET) analogs attenuate cisplatin nephrotoxicity. *FASEB J* 27: 2946–2956, 2013
16. Lindenmeyer MT, Rastaldi MP, Ikehata M, Neusser MA, Kretzler M, Cohen CD, Schlöndorff D: Proteinuria and hyperglycemia induce endoplasmic reticulum stress. *J Am Soc Nephrol* 19: 2225–2236, 2008
17. Ohse T, Inagi R, Tanaka T, Ota T, Miyata T, Kojima I, Ingelfinger JR, Ogawa S, Fujita T, Nangaku M: Albumin induces endoplasmic reticulum stress and apoptosis in renal proximal tubular cells. *Kidney Int* 70: 1447–1455, 2006
18. Mizobuchi N, Hoseki J, Kubota H, Toyokuni S, Nozaki J, Naitoh M, Koizumi A, Nagata K: ARMET is a soluble ER protein induced by the unfolded protein response via ERSE-II element. *Cell Struct Funct* 32: 41–50, 2007
19. Oh-Hashi K, Tanaka K, Koga H, Hirata Y, Kiuchi K: Intracellular trafficking and secretion of mouse mesencephalic astrocyte-derived neurotrophic factor. *Mol Cell Biochem* 363: 35–41, 2012
20. Apostolou A, Shen Y, Liang Y, Luo J, Fang S: Armet, a UPR-upregulated protein, inhibits cell proliferation and ER stress-induced cell death. *Exp Cell Res* 314: 2454–2467, 2008
21. Miner JH, Go G, Cunningham J, Patton BL, Jarad G: Transgenic isolation of skeletal muscle and kidney defects in laminin beta2 mutant mice: Implications for Pierson syndrome. *Development* 133: 967–975, 2006
22. Zinszner H, Kuroda M, Wang X, Batchvarova N, Lightfoot RT, Remotti H, Stevens JL, Ron D: CHOP is implicated in programmed cell death in response to impaired function of the endoplasmic reticulum. *Genes Dev* 12: 982–995, 1998
23. Dong B, Zhou H, Han C, Yao J, Xu L, Zhang M, Fu Y, Xia Q: Ischemia/reperfusion-induced CHOP expression promotes apoptosis and impairs renal function recovery: The role of acidosis and GPR4. *PLoS One* 9: e110944, 2014
24. Yang JR, Yao FH, Zhang JG, Ji ZY, Li KL, Zhan J, Tong YN, Lin LR, He YN: Ischemia-reperfusion induces renal tubule pyroptosis via the CHOP-caspase-11 pathway. *Am J Physiol Renal Physiol* 306: F75–F84, 2014
25. Lindahl M, Danilova T, Palm E, Lindholm P, Vöikar V, Hakonen E, Ustinov J, Andressoo JO, Harvey BK, Otonkoski T, Rossi J, Saarma M: MANF is indispensable for the proliferation and survival of pancreatic β cells. *Cell Reports* 7: 366–375, 2014
26. Cybulsky AV, Takano T, Papillon J, Khadir A, Liu J, Peng H: Complement C5b-9 membrane attack complex increases expression of endoplasmic reticulum stress proteins in glomerular epithelial cells. *J Biol Chem* 277: 41342–41351, 2002
27. Cybulsky AV, Takano T, Papillon J, Bijian K: Role of the endoplasmic reticulum unfolded protein response in glomerular epithelial cell injury. *J Biol Chem* 280: 24396–24403, 2005
28. Inoki K, Mori H, Wang J, Suzuki T, Hong S, Yoshida S, Blattner SM, Ikenoue T, Rüegg MA, Hall MN, Kwiatkowski DJ, Rastaldi MP, Huber TB, Kretzler M, Holzman LB, Wiggins RC, Guan KL: mTORC1 activation in podocytes is a critical step in the development of diabetic nephropathy in mice. *J Clin Invest* 121: 2181–2196, 2011
29. Bek MF, Bayer M, Müller B, Greiber S, Lang D, Schwab A, August C, Springer E, Rohrbach R, Huber TB, Benzinger T, Pavenstädt H: Expression and function of C/EBP homology protein (GADD153) in podocytes. *Am J Pathol* 168: 20–32, 2006
30. Markan S, Kohli HS, Joshi K, Minz RW, Sud K, Ahuja M, Anand S, Khullar M: Up regulation of the GRP-78 and GADD-153 and down regulation of Bcl-2 proteins in primary glomerular diseases: A possible involvement of the ER stress pathway in glomerulonephritis. *Mol Cell Biochem* 324: 131–138, 2009

This article contains supplemental material online at <http://jasn.asnjournals.org/lookup/suppl/doi:10.1681/ASN.2014100986/-/DCSupplemental>.